University of California

Ernest O. Lawrence Radiation Laboratory

GENERALIZED PAIRING IN LIGHT NUCLEI. I. SOLUTIONS OF HFB EQUATIONS IN N = Z EVEN–EVEN NUCLEI

J. Bar-Touv, A. Goswami, A. Goodman, and G. Struble

July 1968

Berkeley, California

DISCLAIMER

Submitted to Physical Review

UCRL-18363
Preprint

UNIVERSITY OF CALIFORNIA

Lawrence Radiation Laboratory
Berkeley, California 94720

AEC Contract No. W-7405-eng-48

GENERALIZED PAIRING IN LIGHT NUCLEI. I. SOLUTIONS OF HFB EQUATIONS IN N=Z EVEN-EVEN NUCLEI

J. Bar-Touv, A. Goswami, A. Goodman, and G. Struble

July 1968

GENERALIZED PAIRING IN LIGHT NUCLEI. I. SOLUTIONS OF HFB EQUATIONS IN N=Z EVEN-EVEN NUCLEI*†

J. Bar-Touv†

Lawrence Radiation Laboratory, University of California
Berkeley, California 94720

and

Case Western Reserve University
Cleveland, Ohio

and

A. Goswami†**

Case Western Reserve University
Cleveland, Ohio

and

A. Goodman and G. Struble

Department of Chemistry and Lawrence Radiation Laboratory
University of California, Berkeley, California 94720

July 1968

ABSTRACT

The HFB equations are solved for the N=Z even-even nuclei in the s-d shell. The possibility of generalized pairing correlations (e.g. both T = 0 and T = 1 pairing) is studied in detail. It is found that the two kinds of pairing are mutually exclusive and that the lowest HFB solution for the even-even N = Z nuclei is of T = 0 independent pairs. The validity and the extent of these correlations is further examined by projecting onto eigenstates of the total number operator. These T = 0 pairing correlation build-up for the axially symmetric prolate Mg^{24} oblate S^{32} and prolate Ar^{36} HFB solution. Studying the relevance of these HFB solutions to the experimental

spectra it is found the HFB field gives a more consistent description of the structure of N = Z even-even nuclei and it can resolve the discrepancies and also the failure of the HF field in the upper half of the s-d shell.

I. INTRODUCTION

Due to the vast amount of experimental data for the s-d shell nuclei this shell has become a testing area for various nuclear structure models. One of the most studied models in this shell is related to the idea of "intrinsic" state. The "intrinsic" state is not the actual state of the nucleus but rather, provides a basis from which physical states can be extracted. The intrinsic state model was first employed using a harmonic oscillator potential to calculate deformed single-particle orbitals.[1,2] Recently the connection between the intrinsic structure of nuclei and the basic two-body interaction has been investigated by utilizing the Hartree-Fock (HF) approximation.[3] A large number of works have already been accumulated regarding the self-consistent fields in the s-d shell nuclei. Originally the HF calculations[4,6] were performed by using an effective central two-body interaction and by confining the single-particle space to a single major shell and thus were quite restricted. More recently complete HF calculations with renormalized realistic interaction and extended shell model space have been performed.[7,8] The majority of these works involve the N = Z even-even nuclei.

The N = Z even-even nuclei are singled out for the theoretical study because of the following features. The ground state equilibrium shape of Ne^{20}, Mg^{24}, Si^{28}, and S^{32} all seem to be deformed. This suggests that these nuclei may definitely be described in terms of deformed intrinsic states. If the Coulomb force is neglected the exchange of protons and neutrons together with time-reversal become symmetries of the self-consistent field and thus bring a considerable simplification to the calculations and the interpretation of the resulting structure.

The major new insight gained by the HF calculations has been the existence of large energy gap between the occupied and unoccupied single-particle levels.[9] This single-particle gap is the main factor in determining the extent to which the HF single-determinant approximation is valid. Its presence lead to a fairly good description of the ground state rotational spectrum by employing projection or cranking techniques. It should be however observed that 1) the HF equations give a large number of solutions for each nucleus most of which do not have large gap, 2) the HF solutions underestimate the spacing between the ground and the excited rotational bands in the first half of the s-d shell, 3) recent analysis of experimental data in Mg^{25} suggests that the intrinsic structure of Mg^{24} should be axially symmetric[10] while the preferred HF state is triaxial, and 4) the simple HF picture is completely unable to explain the structure of the upper half of the s-d shell. The presence of HF solutions with small gaps suggests that these solutions are unstable with respect to higher correlations and that dynamically correlated intrinsic states may in fact be necessary to explain experiment.

A natural generalization of the HF self-consistent field method can be made by taking into account generalized pairing correlations. This is known as the Hartree-Fock-Bogoliubov (HFB) method. It has been known for some time that $J = 0$ pairing among like nucleons is important for describing heavy nuclei but almost all calculations have assumed that the underlying self-consistent field is not affected by the correlations. This same approximation has been assumed for s-d shell nuclei but since neutrons and protons are filling the same orbitals it has been necessary to consider the possibility of proton neutron pairing.

Several groups have studied T = 1 J = 0 charge independent pairing in light nuclei. Also T = 0 pairing has been studied and shown to lead to a coherent pair field and hence to a considerable energy gap for single quasi-particle spectrum.[11] Recently calculations have been reported which consider the possibility of combined T = 0 and T = 1 pairing correlations among the nucleons.[12,13] However, these calculations were incomplete in the sense that the pairing part was separated inconsistently from the underlying intrinsic field. This backward effect is expected to be particularly important when there is a significant dispersion of occupation across the Fermi surface due to pair correlations. To study this effect the HFB method suggests itself as a method which takes the HF and the pairing fields on equal basis.

The first group to perform HFB calculations were Dietrich et al.[14] They studied the structure of deformed rare earth nuclei and also of Mg^{24} assuming only J = 0 pairing between like nucleons. Recently Faessler et al.[26] have performed similar calculations for the 1p and 2s1d shells. The result of these calculations for N = Z nuclei is that this kind of pairing is not an important factor in the structure of these nuclei.

In this paper we examine the effect generalized pairing (including T = 0 independent pairing) on the HFB self-consistent field. In Sect. II we give details of the formalism and discuss an ansatz which allows the separation of the single-particle and the pairing equations. Section III contains a discussion of the nature of the HFB solutions, and the effects of particle number nonconservation. Finally a summary and conclusion are given in Sect. IV.

II. HF AND HFB METHODS

II.1. Equation of Motion, HF and HFB Factorizations

We start with the Hamiltonian

$$H = \sum e_{i\mu} C_{i\mu}^{\dagger} C_{i\mu} + \frac{1}{4} \sum \langle i\mu\ j\nu | V_a | k\rho\ \ell\sigma \rangle\ C_{i\mu}^{\dagger} C_{j\nu}^{\dagger} C_{\ell\sigma} C_{k\rho} \qquad (1)$$

where $C_{i\mu}^{\dagger}$, $C_{i\mu}$ are creation and annihilation in the n, ℓ, j, m, μ representation (μ denotes z component of isospin), e_i denotes the single particle shell model energy, and V is the two nucleon interaction.

The commutator of $C_{i\mu}^{\dagger}$ with H is given by

$$\left[H, C_{i\mu}^{\dagger}\right] = e_{i\mu} C_{i\mu}^{\dagger} + \frac{1}{2} \sum \langle k\rho\ \ell\sigma | V_a | i\mu\ j\nu \rangle\ C_{k\rho}^{\dagger} C_{\ell\sigma}^{\dagger} C_{j\nu} \qquad (2)$$

The equation of motion method consists in linearizing this equation by using Wick's theorem and neglecting the normal ordered term:

$$C_{k\rho}^{\dagger} C_{\ell\sigma}^{\dagger} C_{j\nu} = N(C_{k\rho}^{\dagger} C_{\ell\sigma}^{\dagger} C_{j\nu}) + \langle C_{\ell\sigma}^{\dagger} C_{j\nu} \rangle C_{k\rho}^{\dagger}$$

$$- \langle C_{k\rho}^{\dagger} C_{j\nu} \rangle C_{\ell\sigma}^{\dagger} + \langle C_{k\rho}^{\dagger} C_{\ell\sigma}^{\dagger} \rangle C_{j\nu} \qquad (3)$$

The normal product term is neglected in both HF and HFB methods. An a postiori justification can be given if there is a large energy gap in the single (quasi)particle spectrum in the HFB or HF representation.

The HF factorization consists in writing

$$C_{k\rho}{}^{\dagger}C_{\ell\sigma}{}^{\dagger}C_{j\nu} = \langle C_{\ell\sigma}{}^{\dagger}C_{j\nu}\rangle C_{k\rho}{}^{\dagger} - \langle C_{k\rho}{}^{\dagger}C_{j\nu}\rangle C_{\ell\sigma}{}^{\dagger} \tag{4}$$

This corresponds to the minimization of the Hamiltonian in a single detrimental wave function.

The HFB factorization consists in including the extra term $\langle C_{k\rho}{}^{\dagger}C_{\ell\sigma}{}^{\dagger}\rangle C_{j\nu}$ from Eq. (3). The major consequences of this is the nonconservation of the particle number and isospin. It is equivalent to minimization of the Hamiltonian in a BCS type wave function which is a particular combination of determinants.

II.2. The HF Basis

With HF factorization the equation of motion becomes

$$\left[H, C_{i\mu}{}^{\dagger}\right] = \sum_{k} \mathcal{H}_{i\mu\ k\mu} C_{k\mu}{}^{\dagger} \tag{5}$$

$$\text{where } \mathcal{H}_{i\mu\ k\mu} = e_i \delta_{ik} + \sum \langle k\mu\ \ell\nu | V_a | i\mu\ j\nu\rangle \langle C_{\ell\nu}{}^{\dagger} C_{j\nu}\rangle \tag{6}$$

which for N = Z nuclei is independent of the isospin index μ.

The HF representation is obtained by observing that when one assumes the HF factorization an eigen mode of the system can be written

$$C_{\alpha\mu}{}^{\dagger} = \sum_{i} a^{\alpha}{}_{i} C_{i\mu}{}^{\dagger} \quad . \tag{7}$$

The coefficients in the transformation are obtained by solving the eigenvalue equation

$$\mathcal{H}|\alpha\mu\rangle = \varepsilon_\alpha|\alpha\mu\rangle \quad . \tag{8}$$

ε_α defines the HF single particle energies. The HF total energy is given by

$$E_{HF} = \langle H\rangle_{HF} = \frac{1}{2}\sum_\alpha \{\langle\alpha|t|\alpha\rangle + \varepsilon_\alpha\} \tag{9}$$

where

$$\langle i\mu|t|j\nu\rangle = e_i\,\delta_{ij}\delta_{\mu\nu} \tag{10}$$

Some general properties of the solutions of the HF equations for even-even N = Z nuclei in the s-d shell which we assume are 1) symmetry under the exchange of neutron and proton and 2) the time reversal invariance. We define here the time reversed single particle state as

$$|\bar{\alpha}\rangle = \sum_i a^\alpha{}_i(-1)^{j_i-m_i}|j_i-m_i\rangle \tag{11}$$

The ground HF solution corresponds to the lowest minimum. This solution has always been found to possess a large gap between occupied and unoccupied states. This gap does not allow the building up of the pair field in the BCS sense.

Besides the ground state solution, other solutions of the HF equations are found which sometimes differ little in $\langle H\rangle$. Most of these higher solutions have a less conspicuous single particle gap and therefore are more susceptible to the inclusion of the pairing correlations. We shall consider a self-consistent treatment of pairing based on these HF solutions. The

pairing correlations are expected to establish the required gap in the single quasiparticle spectrum and thus bring stability to the new self-consistent field.

II.3. Treatment of the Pair Field and the HFB Factorization

We have

$$\left[H, C_{i\mu}^{\dagger}\right] = \sum \mathcal{H}_{i\mu\ k\mu} C_{k\mu}^{\dagger} + \sum \Delta_{i\mu\ k\nu} C_{k\nu} \tag{12}$$

where

$$\Delta_{i\mu\ k\nu} = \frac{1}{2} \sum \langle j\rho\ell\sigma | V_a | i\mu k\nu \rangle \langle C_{j\rho}^{\dagger} C_{\ell\sigma}^{\dagger} \rangle \tag{13}$$

Similarly we can write down the analogous equation of motion for $C_{i\mu}$. The HFB method consists in the self-consistent diagonalization of H in the extended single particle basis of $C_{i\mu}^{\dagger}$, $C_{i\mu}$

$$\begin{pmatrix} \mathcal{H} & \Delta \\ \Delta^{+} & -\tilde{\mathcal{H}} \end{pmatrix} \tag{14}$$

to obtain the eigen modes of the system.

We shall solve the HFB equations under the following constraints:

The different HF bases obtained when Δ is set equal to zero are assumed to make Δ diagonal in the space spin part of each of the single particle orbitals. Also the pairing matrix is assumed to connect a single particle operator $C_{\alpha}^{\dagger}$ to its time reversal conjugant $C_{\bar{\alpha}}$ (this follows from the assumed

time reversal invariance of the resulting ground state). With this assumption the HFB matrix is reduced to submatrices, each submatrix of dimension 4×4 belonging to one single particle orbital.

The HFB submatrix belonging to an HF orbital α can be written as

$$\begin{pmatrix} \underline{\varepsilon}_\alpha & \underline{\Delta}_\alpha \\ \underline{\Delta}_\alpha & -\underline{\varepsilon}_\alpha \end{pmatrix} \tag{15}$$

where

$$\underline{\Delta}_\alpha = \begin{pmatrix} \Delta_{pp}(\alpha) & \Delta_{pn}(\alpha) \\ \Delta_{pn}(\alpha) & \Delta_{nn}(\alpha) \end{pmatrix} \tag{16}$$

$$\underline{\varepsilon}_\alpha = \begin{pmatrix} \varepsilon_\alpha & 0 \\ 0 & \varepsilon_\alpha \end{pmatrix}$$

By a proper choice of phases we choose $\Delta^\dagger = \Delta$. Also we can assure $\Delta_{np}(\alpha) = \Delta_{np}^{T=1}(\alpha) + i\Delta_{np}^{T=0}(\alpha)$ as pointed out in Ref. (12). This identification of the real and imaginary parts of Δ_{np} allows us to separate the role of the $T = 1$ and $T = 0$ forces in a simple manner. The success of the HFB method depends crucially on whether there is an energy gap in the quasi particle spectrum. There exist the following possibilities for having such a gap.

1) If $\Delta_{np} = 0$, the eigenvalue for matrix (15) equations are reduced to independent BCS equations for the protons and neutrons where the quasiparticle energies are

$$E_\alpha = \sqrt{\varepsilon_\alpha^2 + \Delta_{pp}^2(\alpha)} \tag{17}$$

with an energy gap of Δ_α. Note that ε_α is measured relative to the chemical potential λ. This is the case for heavy nuclei with large neutron excess.

2) If $\Delta_{pp} = \Delta_{nn} = \Delta_{np}^{T=1} = 0$ then the matrix (15) is again reduced to 2×2 matrices with the energy eigenvalue

$$E_\alpha = \sqrt{\varepsilon_\alpha^2 + \Delta(\alpha)_{np}^{T=0\ 2}} \tag{18}$$

with an energy gap $\Delta(\alpha)_{np}^{T=0}$. This is the case of isospin pairing.[11]

3) $\underline{\Delta}\underline{\Delta}^\dagger$ = constant $\times$ $\underline{I}$, $\underline{I}$ being the unit matrix. Since $\Delta^\dagger = \Delta$,

$$\Delta^2 = |\text{Det } \underline{\Delta}|\underline{I} \tag{19}$$

In this case the energy eigenvalue is given by

$$E_\alpha = \sqrt{\varepsilon_\alpha^2 + |\text{Det } \underline{\Delta}_\alpha|} \tag{20}$$

with an energy gap of $|\text{Det } \underline{\Delta}_\alpha|$. Since the ground state of most N = Z nuclei has T = 0, one would like the T = 0 state to be contained in the intrinsic state without confining the solutions to be eigenstates of T^2. In analogy to HF where one constrains $\langle \underline{J} \rangle$ to be zero we impose the condition $\langle \underline{T} \rangle = 0$, that is all components of the isospin vanish in the ground state on the average. We thus guarantee more degrees of freedom in the isotopic spin coordinates allowing the possibility for intrinsic states having lower energy. The condition (19) then follows. Note that the case 2 is a special case of this more general solution. The gap and number equation in the general case

are given as

$$\Delta_{pp}(\alpha) = -\Delta_{nn}(\alpha) = \sum \langle \alpha\bar{\alpha}\ T = 1 | V_a | \gamma\bar{\gamma}\ T = 1 \rangle \frac{\Delta_{pp}^{T=1}(\gamma)}{E_\gamma}$$

$$\Delta_{np}^{T=1}(\alpha) = \sum \langle \alpha\bar{\alpha}\ T = 1 | V_a | \gamma\bar{\gamma}\ T = 1 \rangle \frac{\Delta_{np}^{T=1}(\gamma)}{E_\gamma} \qquad (21)$$

$$\Delta_{np}^{T=0}(\alpha) = \sum \langle \alpha\bar{\alpha}\ T = 0 | V_a | \gamma\bar{\gamma}\ T = 0 \rangle \frac{\Delta_{np}^{T=0}(\gamma)}{E_\gamma}$$

$$N = Z = \sum \left(1 - \frac{\varepsilon_\alpha - \lambda}{E_\alpha}\right) ; \quad = \lambda = \text{chemical potential} \qquad (22)$$

The generalized Bogoliubov transformation corresponding to this simplified HFB problem is given as

$$\begin{pmatrix} a_{\alpha 1}^{\dagger} \\ a_{\alpha 2}^{\dagger} \\ a_{\bar{\alpha} 1} \\ a_{\bar{\alpha} 2} \end{pmatrix} = \begin{pmatrix} u_\alpha & 0 & -V_\alpha & -V'_\alpha \\ 0 & u_\alpha & -V'^{*}_\alpha & V_\alpha \\ V_\alpha & V'_\alpha & u_\alpha & 0 \\ V'^{*}_\alpha & -V_\alpha & 0 & u_\alpha \end{pmatrix} \begin{pmatrix} C_{\alpha p}^{\dagger} \\ C_{\alpha p}^{\dagger} \\ C_{\bar{\alpha} p} \\ C_{\bar{\alpha} n} \end{pmatrix} \qquad (23)$$

where u_α and V_α are real and v'_α is complex. The occupation probability of the level α is

$$V_\alpha^2 = v_\alpha^2 + |v'_\alpha|^2 \qquad (24)$$

Dietrich et al.[14] have shown that to a good approximation the principal effect of pairing on the HF degrees of freedom is accounted for in the dispersion of

the occupation across the Fermi surface. This suggests the following ansatz for solving the HFB equations. First solve the HF problem with occupation number of 1 or 0 for a particular orbital; then solve the BCS problem separately to extract improved occupation numbers, solve the HF equations again with these new occupations, and repeat the last two steps until convergence is obtained. The Hartree-Fock equations become;

$$\mathcal{H}(V^2)\ |\alpha\rangle = \varepsilon_\alpha |\alpha\rangle \tag{25}$$

with

$$|\alpha\rangle = \sum_i a_i^\alpha(v^2)\ |i\rangle \tag{26}$$

and

$$\mathcal{H}_{i\mu\ k\mu}(V^2) = e_i\delta_{ik} + \sum \langle i_\alpha\alpha|V_a|k\alpha\rangle\ V_\alpha^2 \tag{27}$$

The ground state energy in the HFB approximation can be written as a sum of an 'analogous' HF energy and the pairing energy.

$$\langle H\rangle = E_{HF} + E_{pair} \tag{28}$$

$$E_{HF} = \frac{1}{2}\sum_\alpha \left(\sum_i e_i a_i^{\alpha 2} + \varepsilon_\alpha\right)\ V_\alpha^2 \tag{29}$$

$$E_{pair} = 2\sum_{\alpha>0} \Delta_{pp}(\alpha)\ u_\alpha v_\alpha + \Delta_{np}^{T=1}(\alpha)\ u_\alpha \mathrm{Re}\ v'_\alpha + \Delta_{np}^{T=0}\ u_\alpha\ \mathrm{Im}\ v'_\alpha \tag{30}$$

Note that we have used the same notation for the energy and wavefunctions of the HF Hamiltonian even when occupation other than zero and one have been used.

III. NATURE OF THE SOLUTIONS OF THE HFB EQUATIONS

In this section we study the general nature of the solutions of the HFB equations for s-d shell N = Z nuclei. Our contention is that for deriving the major features of the HFB field we can use a simple central two-body interaction which is chosen to be the Rosenfeld force with a Yukawa radial shape

$$V = V_0 \frac{e^{-\gamma/a}}{\gamma} (0.3 + 0.7\ \underline{\sigma}_1 \cdot \underline{\sigma}_2) \tag{31}$$

$$a = 1.35f; \quad v_0 = 50 \text{ MeV}$$

This force has been used extensively in earlier HF studies. We confine ourselves to the s-d shell with an oscillator parameter of 1,65 fermi. The single particle part of the Hamiltonian has been chosen to be of the form

$$e_i = e_o + \alpha_{\ell\cdot s} \langle i|\ell\cdot s|i\rangle + \alpha_{\ell^2} \langle i|\ell^2|i\rangle \tag{32}$$

In particular we will refer to the two following cases. $\alpha_{\ell^2} = 0$ Mev, $\alpha_{\ell\cdot s} = -2.8$ MeV, and $\varepsilon_0 = -4.2$ MeV used in Ref. (6) and $\alpha_{\ell^2} = 0.2$, $\alpha_{\ell\cdot s} = -2.0$ and $\varepsilon_0 = -3.3$ MeV corresponding to the experimental single particle energy spectrum of O^{17}.

III.1. Tendency to Higher Symmetry

One major feature of pairing correlations is the tendency toward higher symmetry of the intrinsic wave function. For example, it is well

known that the J = 0 pairing correlations are responsible for the sphericity of a large number of open shell nuclei.[15] For deformed nuclei in the rare earth region, pairing correlations lead to axial symmetry.[16]

In the s-d shell, HF calculations have shown that the ground HF solution corresponds to axially asymmetric shapes for the nuclei Mg^{24} and S^{32}. The HF equations usually possess several solutions for each nucleus which often differ very little in the HF energy, i.e. $\langle H \rangle$. The criterion usually adopted in picking the HF ground state viz lowest value of $\langle H \rangle$ is not very meaningful since neglected correlations, for example pairing, would lower the energy of the other solutions considerably. Moreover, the reliability of the minimum $\langle H \rangle$ criterion is further affected by 1) second order HF energy, 2) rotational energy, and 3) zero point fluctuation energy. In particular, the first effect is found to be large, about 17% of the first order HF potential energy.[8] For Mg^{24} and S^{32} there exists axially symmetric* solutions which differ in $\langle H \rangle$ from the axially asymmetric solutions by about 3 MeV. The single particle HF gaps for these axially symmetric solutions are 3.0 MeV for Mg^{24} and 5.3 MeV for S^{32}. The gaps for the triaxial solutions however are 7.4 MeV and 6.6 MeV respectively. (These values are for $\alpha_{\ell \cdot s} = -2.8$ MeV.) The single particle gap for the triaxial solutions turns out to be large

---

*The axially symmetric HF solution for S^{32} and Ar^{36} which favors pairing correlations are different from the ones given in Ref. (6). This HF solution is given in Table III.

enough to exclude pairing in the BCS sense. This does not mean that pairing correlations do not exist in these cases. The BCS equations are well known to have a cutoff in the build-up of the pairing correlations. The fact that the pairing correlations are small in the axially asymmetric state is basically due to the fact that axial asymmetry has already taken care of a major part of the dispersion of the occupation above the fermi level relative to the axially symmetric solution.[17] The axially asymmetric solution could also be used as a basis for the inclusion of pairing correlations but at the expense of using more elaborate techniques, namely number conserving representation. The defect of such an approach is the nonexistence of simple modes of excitation. The HFB solutions corresponding to the axially symmetric shapes are shown in Table I. After the energy gain by pairing correlations is taken into account along with the rotational energy, the $\langle H \rangle$ for the axially symmetric state becomes comparable to that of the triaxial solution. It will be shown in Sect. III.3 that the paired solution is likely to be closer to the physical intrinsic state on the basis of comparison with experiment. In this sense only pairing restores axial symmetry to Mg^{24} and S^{32}.

Another interesting example of this tendency toward higher symmetry caused by the pairing correlation occurs for the triaxial HF basis of Ne^{20}. The HFB solution is given in Table II. Notice that the dispersion of the occupation due to the pairing correlation is such that all the m states of the $d_{5/2}$ orbital are almost equally occupied, i.e., the intrinsic state has become spherical. The small deviation from sphericity is due to the fact that this solution corresponds to combined T = 0 and T = 1 pairing and that T = 0 pairing inherently implies deformation. It is not clear if this solution corresponds to any physical excited state of Ne^{20}.

III.2. Prolate Versus Oblate Shapes

Another feature of the lowest axially symmetric HF solution for the s-d shell is that one gets prolate shapes for the lower half of the shell and oblate shapes for Si^{28} and the upper half. For all s-d shell nuclei there are other HF symmetric solutions of opposite shape.

However, in analogy to the competition between axially symmetric and asymmetric shapes, these axial solutions may differ little in $\langle H \rangle$, but one, by virtue of a small gap, may allow extensive pairing correlations. This is the case for Ar^{36} where the prolate and oblate solutions differ in $\langle H \rangle$ by only 3 MeV. The single particle gap for the prolate solution is 2.4 MeV compared to 7.4 MeV for the oblate solution. Consequently, the energy gain due to pairing for the prolate state makes the $\langle H \rangle$ closer for the two states. Table I displays the HFB solution corresponding to the prolate state. The physical relevance of the paired solution will be discussed in Sect. III.6.

III.3. Effect of Self-Consistency on the HF and Paired Field

In this section we shall study the effects of the pair field on the HF field and vice versa. Table III shows the HF wave function for the cases of S^{32} and Ar^{36} with zero pairing and for the final self-consistent HFB solution ($\ell \cdot s$ force strength is -2.8 MeV). The change in the HF field due to pairing depends very much on the amount of dispersion of the occupation across the fermi surface which in its turn depends on the single particle gap. In Mg^{24} and S^{32} where the dispersion was rather small the change in the HF field, due to the pair correlations is small. Significant change, however, occurs in the total HF energy of the system which decreases due to the dispersion of the

occupation to the unoccupied single particle states of lower binding energy. This loss is more than compensated by the large gain in pairing energy. Moreover, there is an extra gain in the rotation energy due to a decrease in the moment of inertia (see Sect. III.6). In Ar^{36} where the dispersion is particularly large the resulting changes in the HF and HFB fields will single out Ar^{36} from other N = Z even-even nuclei as will be discussed in Sect. III.6.

In order to study the effect of the HF field on pairing in a meaningful way, we vary the single-particle $\ell \cdot s$ force strength. As expected, the decrease of the HF single-particle gap brings an increase in the dispersion across the fermi surface due to pairing and hence an increase in the pairing energy. Table IV shows the variation of various quantities of the self-consistent fields as a function of $\ell \cdot s$ force strength. In general the HFB quantities show a relative stability compared to those of the relevant HF fields. In particular the quasiparticle gap (the unperturbed energy of the K = 2+ state) is significantly stable compared to the abrupt changes of the HF single-particle gap.

It is interesting to notice here that the main effect of using the realistic forces and the extension of the shell model space to include all lower shells is the reduction of the single particle HF gap.[7] This is particularly prominent for the axial symmetric HF solutions of Mg^{24} and S^{32} considered in this paper. For example, in Mg^{24} the gap reduces to 0.5 MeV compared to 3.1 MeV used in this paper.[18] With the help of Table IV it is easy to extrapolate the expected changes in the pairing correlations due to the realistic forces. The most significant change except the obvious increase in pairing due to the lower HF gap may well occur in the reduction of HF energy loss due to pairing which should be much less than we have found here.

III.4. T = 0 Versus T = 1 Pairing

One consistent feature of the generalized pairing solutions for the N = Z even-even nuclei is the mutual exclusion of T = 0 and T = 1 pairing; i.e., no physical cases show simultaneous T = 0 and T = 1 pairing. This result does not mean that the T = 1 (T = 0) pair correlation is identically 0 for T = 0 (T = 1) pairing, but being small they cannot be accounted for in BCS. It is well known that BCS solutions go to the trivial ($\Delta = 0$) solution in the small Δ limit.

For the even-even nuclei due to the large separation of the T = 0 and T = 1 states, as seen in the experimental spectrum, isospin conservation should be important and therefore the T = 0 pairing solutions are to be accepted as the physical solutions. The T = 1 pairing solution gives an isospin intrinsic state out of which one can project the various T states. However, it is unlikely that states separated by $\sim$9 MeV could be contained in the same intrinsic state.[19] For this reason, we disregard the T = 1 pairing solution. In the T = 0 pairing picture of the ground state, the T = 1 states are to be generated as two quasiparticle pairs coupled to T = 1.

III.5. Projections onto Eigenstates of the Number Operator

As mentioned in II.2 the HFB vacuum is not an eigenstate of the number operator. The effects of this approximation have been extensively studied in heavy nuclei where only TZ = 1 pairing occurs.[14] However such studies have not been performed for T = 0 pairing and for realistic systems with small numbers of nucleons.

The canonical HFB approximation has the conceptual advantage of considering the variational problem in two parts, first solving the Euler-Lagrange equations for the Hartree-Fock degrees of freedom, and then solving the pairing part for the best set occupation parameters for the Hartree-Fock orbitals. When the solutions to the HFB equations give pure T = 0 or TZ = 1 solutions, then the pairing equations result from a variation with the trial wavefunctions

$$\psi_{T=0} = \prod_{\substack{\alpha>0 \\ \tau}} (u_\alpha + (-1)^{1/2-\tau}\, i v_\alpha\, C^\dagger_{\alpha\tau}\, C^\dagger_{\bar{\alpha}-\tau})|0\rangle \tag{33}$$

$$\psi_{TZ=1} = \prod_{\alpha>0} (u_\alpha + v_\alpha\, C^\dagger_{\alpha\frac{1}{2}}\, C^\dagger_{\bar{\alpha}\frac{1}{2}}) \prod_{\alpha>0} (u_\alpha + v_\alpha\, C^\dagger_{\alpha-\frac{1}{2}}\, C^\dagger_{\bar{\alpha}-\frac{1}{2}})|0\rangle \tag{34}$$

In these restricted cases the u's and v's may be taken to be real numbers. Since all physically interesting solutions for even-even nuclei are T = 0, we shall present the relevant equations for the T = 0 case only.

Having written a trail wavefunction for the number nonconserving part of the variational problem, we can correct the defect by projecting out that part of ψ which contains the proper number of nucleon pairs. We may express this formally as

$$\psi_{T=0} = C\oint d\xi\, \xi^{-n_0-1} \prod_{\substack{\nu>0 \\ t}} (u_\nu + \xi(-1)^{1/2-\tau}\, i v_\nu\, C^\dagger_{\nu\tau}\, C^\dagger_{\nu-\tau})|0\rangle \tag{35}$$

where C is the normalization constant and is given by

$$|C|^2 = -1/4\pi^2 R_0^0 \tag{36}$$

n_0 is the number of neutron proton pairs, and the

$$R_n^N(\nu_1,\ldots,\nu_N) = \frac{1}{2\pi i} \oint dz z^{-(n_0-n)-1} \prod_{\nu\neq\nu_1\ldots\nu_N} (u_\nu^2 + z v_\nu^2)(u_\nu^2 + z v_\nu^2) \tag{37}$$

and are called residuum integrals. Taking the expectation value of (1) in (33), we find the energy is given by

$$\begin{aligned} E = & \sum_{\nu_1} \tilde{\varepsilon}_{\nu_1} v_{\nu_1}^2 R_1^1(\nu_1)/R_0^0 \\ & + \sum_{\nu_1\nu_2} H_{\nu_1\nu_2} v_\nu^2 v_\nu^2 R_2^2(\nu_1\nu_2)/R_0^0 \\ & + \sum_{\nu_1\nu_2} P_{\nu_1\nu_2} u_{\nu_1} v_{\nu_1} u_{\nu_2} v_{\nu_2} R_1^2(\nu_1\nu_2)/R_0^0 \end{aligned} \tag{38}$$

where

$$\tilde{\varepsilon}_\nu = 4\langle\nu|t|\nu\rangle + \langle\nu\bar{\nu}|V_a|\nu\bar{\nu}\rangle_{T=0} \tag{39}$$

$$\begin{aligned} H_{\nu_1\nu_2} = & 3[\langle\nu_1\nu_2|V_a|\nu_1\nu_2\rangle_{T=1} + \langle\nu_1\bar{\nu}_2|V_a|\nu_1\bar{\nu}_2\rangle_{T=1}] + \\ & [\langle\nu_1\nu_2|V_a|\nu_1\nu_2\rangle_{T=0} + (-1)^{\delta_{\nu_1\nu_2}}\langle\nu_1\bar{\nu}_2|V_a|\nu_1\bar{\nu}_2\rangle_{T=0}] \end{aligned}$$

and

$$P_{\nu_1\nu_2} = 2\langle\nu_1\bar{\nu}_1|V_a|\nu_2\bar{\nu}_2\rangle_{T=0}(1 - \delta_{\nu_1\nu_2}) \tag{41}$$

Variation of the energy with respect to the v's gives the set of equations

$$(\hat{\varepsilon}_\alpha + \Gamma_\alpha + \Lambda_\alpha)\, u_\alpha v_\alpha + \frac{1}{2}\Delta_\alpha(u_\alpha^2 - v_\alpha^2) = 0 \tag{42}$$

where

$$\hat{\varepsilon}_\alpha = \frac{1}{2}\tilde{\varepsilon}_\alpha\, R_1^1(\alpha)/R_0^0 \tag{43}$$

$$\Gamma_\alpha = \sum_{\nu_1} H_{\alpha\nu_1}\, v_{\nu_1}^2\, R_2^2(\nu_1\alpha)/R_0^0 \tag{44}$$

$$\Delta_\alpha = \sum_{\nu_1} P_{\alpha\nu_1}\, u_{\nu_1} v_{\nu_1}\, R_1^2(\nu_1\alpha)/R_0^0 \tag{45}$$

$$\begin{aligned}\Lambda_\alpha = {} & \frac{1}{4}\sum_{\nu_1}\sigma(\alpha\nu_1)\,\hat{\varepsilon}_{\nu_1}\, v_{\nu_1}^2\,\frac{[R_1^2(\nu,\alpha) - R_1^2(\nu,\alpha)]}{R_0^0} \\ & + \frac{1}{4}\sum_{\nu_1\nu_2}\sigma(\alpha\nu_1\nu_2)\, H_{\nu_1\nu_2}\, v_{\nu_1}^2\, v_{\nu_2}^2\,\frac{[R_3^3(\nu_1\nu_2\alpha) - R_2^3(\nu_1\nu_2\alpha)]}{R_0^0} \\ & + \frac{1}{4}\sum_{\nu_1\nu_2}\sigma(\alpha\nu_1\nu_2)\, P_{\nu_1\nu_2}\, u_{\nu_1} v_{\nu_1}\, u_{\nu_2} v_{\nu_2}\,\frac{[R_2^3(\nu_1\nu_2\alpha) - R_1^3(\nu_1\nu_2\alpha)]}{R_0^0} \\ & - \frac{1}{2}E\,\frac{R_1^1(\alpha) - R_0^1(\alpha)}{R_0^0}\end{aligned}$$

$$\sigma(\alpha\nu_1\ldots\nu_N) = \begin{bmatrix} 4 & \alpha \neq \{\nu_1\ldots\nu_N\} \\ 2 & \alpha = \nu_1 \quad \nu_i\{\nu_1\ldots\nu_N\} \\ 0 & \alpha = \nu_i = \nu_j \quad \nu_i,\ \nu_j\{\nu_1\ldots\nu_N\} \end{bmatrix}$$

Like the BCS equations the potentials in (42) depend on the solutions and so they must be solved by an iterative self consistent procedure. We intend to examine the solutions to these equations in more detail in a future publication and so here we will give only the one numerical example.

Previous investigations suggest the certain features to be expected from such an approach:

1. If we choose as the initial guess the solution to (15), then for the first iteration, Eq. (42) describes the BCS solution with the correct particle number projected out (PBCS). The solutions to (42) always give a lower energy than this solution (FBCS).

2. No matter how large the HF gap or how weak the pairing interaction, there are non-trivial solutions to (42).

3. In the limit, where BCS predicts uniform occupation (strong pairing), FBCS gives smaller dispersion while the limit where BCS gives the gives the trivial solution (weak pairing), the FBCS will always give finite dispersion.

In order to illustrate the effects of number conservation we will examine Mg^{24}, using the protate HF solution (see Table I) for the single particle basis in (15), and T = 0 pairing solution as the initial guess for Eqs. (42). The HF energy is -74.605 MeV which is to be compared to -77.340 MeV for BCS, -76.430 MeV for PBCS, and -76.952 MeV for FBCS. In Fig. 1 we show the effect on the occupation of the six four-fold degenerate orbitals.

Referring to this FBCS solution as a typical example for N = Z even even nuclei, we observe that the considerable gain in ground state energy due to T = 0 independent pairs is preserved in the good N scheme. This demonstrates that the HFB results are not made spurious due to the mixing of the neighboring nuclei. Our results also reflect the above mentioned features. In particular it should be noted, the dispersion is substantially reduced due to number projection. However the number projection does <u>not</u> bring new dynamical

correlations hence the HFB solution is a good intrinsic state and reproduces ground state properties. For expectation values of operators sensitive to the occupation numbers (e.g., stripping spectroscopic factors) this result implies projection is crucial.

III.6. Moment of Inertia

In this section we shall discuss the effect of pairing correlations on the cranking value of moment of inertia. The results of HF calculations (with $\ell\cdot s$ force strength of -2.8 MeV) give fair agreement to the experimental value for Ne^{20} and also for Mg^{24} when axial asymmetry is allowed for.

It has been mentioned before that with the two body force used in this paper, pairing correlations do not build up for Ne^{20} and Si^{28}. We shall, therefore, confine our discussion to Mg^{24}, S^{32}, and Ar^{36}. With the HFB wave function, the only moment of inertia is given by

$$\mathcal{J} = 2 \sum_{\substack{\alpha'>0 \\ \text{all } \alpha}} \frac{|\langle\alpha|j_x|\alpha'\rangle|^2}{E_\alpha + E_{\alpha'}} (u_\alpha|v_{a'}|-u_{\alpha'}|v_a|)^2$$

HFB correlations on the axially symmetric HF basis already given in Sects. I and II for all three nuclei tend to decrease the moment of inertia significantly. Table IV shows the effect of pairing on the moment of inertia parameter $(A = \hbar^2/2\mathcal{J})$ for the axially symmetric state of Mg^{24} for different values of the $\vec{\ell}\cdot\vec{s}$ strength. It is to be noticed that the HF and the HFB moment of inertia parameters show opposite trends with regard to $\alpha_{\ell\cdot s}$. For $\alpha_{\ell\cdot s}$ which corresponds to O^{17} $\ell\cdot s$ splitting the ratio between the HFB and the HF values is more than 2 and as expected this ratio should drop

to 1 when the increased $\underset{\sim}{\ell}\cdot\underset{\sim}{s}$ strength reproduces an HF gap which brings the cutoff in the pairing correlations. A comparison between the moments of inertia parameters of the unpaired axially asymmetric HF solutions and the corresponding axially symmetric HFB solution for Mg^{24} and S^{32} for the two choices of shell model single particle energies used in the present study is given in Table V. A comparison of these values with those presented in Fig. 1 for $\alpha_{\ell\cdot s} = -2.8$ MeV reflects more stability for the HFB moments of inertia over the HF asymmetric values.

The HFB results (including the limiting cases of zero pairing for Si^{28} and Ne^{20}) for the moment of inertia parameter are shown in Fig. 1 along with the experimental values. The experimental values of Ne^{20}, Mg^{24}, and Ar^{36} have been chosen as average values calculated from 0+ - 2+ and 2+ - 4+ spacing. The values of Si^{28} and S^{32} are extracted from the 4+ - 2+ spacing only. The 0+ states of these two nuclei are lowered to their observed positions by their interaction with the first excited 0+ states which correspond to spherical shapes observed at 4.97 and 3.78 MeV respectively in these two nuclei.[20*] The theoretical HFB values for the moment of inertia parameter

---

*The reference to S^{32} as being deformed in the ground state may not be so apparent from the energy spectrum alone. However the large similarity of the angular correlations pattern of pp' reaction[21] in S^{32} and in Si^{28} whose ground state deformation is apparent already from the clear rotational nature of its low lying spectrum suggests that S^{32} can also be looked upon as being deformed. It is however true that there is a particularly big component of the spherical state in the S^{32} ground state and the adopted point of view might just be a question of taste.

are always overestimated which is particularly desirable due to the expected reduction of the cranking estimate due to the Peirls' correction[22] not included here.

The preference of the HFB axially symmetric solution over the unpaired HF axially asymmetric solution for Mg^{24} suggested in the present study is supported by experimental data on stripping spectroscopic factors[23] and also γ branching ratio[24] of Mg^{25}. These experimental data of Mg^{25} favors an axially symmetric shape for the Mg^{24} even-even core. Also the HF asymmetric rotation of Mg^{24} underestimates the spacing between the ground state K = 0 rotational band and the first K = 2 excited band at least by 1 MeV. The HFB unperturbed K = 2 band head being related to the lowest K = 2 two quasiparticle state over estimates this spacing in about 1 MeV (see Table IV) by this is favorable due to expected lowering by the residual interaction between the quasiparticles of the K = 2 subspace.

Of special interest is the case of Ar^{36} where the cranking value of the moment of inertia parameter is found to be 2.84 MeV for the paired prolate state. Such a high value implies that the excitation energy of the rotational states is much bigger than that of the vibrational states of the almost spherical Ar^{36}. Experimentally Ar^{36} spectrum resembles a pure vibrational spectrum. However a close check of experimental BE2 ratios reflect a large amount of unharmonicity characteristic to a transitional nucleus.

Apart from the pairing energy gain already mentioned, the significant increase of the HFB moment of inertia parameter brings another considerable energy gain due to large rotational energy. The energy of the J = 0 band head is given as $E(J = 0) = \langle H \rangle - A\langle J^2 \rangle$ (the value of $\langle J^2 \rangle$ does not change

appreciably). Thus the rotational energy gain $\sim(A_{HFB} - A_{HF}) \langle J^2 \rangle$ with proper choice of $\ell \cdot s$ strength could be considerable and thus bring closer the axially symmetric paired solution and the unpaired axially asymmetric solution.

IV. SUMMARY AND CONCLUSIONS

We have considered the effect of generalized pairing correlations in the N = Z even-even nuclei of the s-d shell by solving the HFB equations. It is well known that the HF equations given several solutions. The usual criterion of choosing among these solutions viz. the lowest value of $\langle H \rangle$ is not meaningful because they differ often only slightly (about 1% of the first order potential energy), whereas the second order HF potential energy is ∿17% of the first order potential energy. Moreover, the energy fluctuation $\langle H^2 \rangle - \langle H \rangle^2$ on the lowest HF solution as well as the higher one is large except for Ne^{20} axially symmetric state.[25] This shows that even the lowest HF solutions are not good approximations to the actual ground state of the system. In view of this, we assert that the HF solutions should be regarded only as basis for further calculations, for example pairing correlations. Only when the higher correlations have been taken into account and the energy calculated to all significant orders can one make a meaningful choice of the proper solution. Alternatively one can try to make such a selection on the basis of experimental data.

In this paper we attempt to study the broad features of the HFB field with the usual choice of the truncated s-d shell space and phenomenological effective two body interaction. The HFB solutions thus derived have been compared with the HF solutions and also with the experimental data. More definitive considerations are under investigation and will be presented in a future publication.

The solutions of the HFB equations are obtained by constraining the pairing matrix Δ to be diagonal in the HF basis (only in the space spin

variables). We have restricted ourselves to N = Z even-even nuclei where the further constrain $\langle \underline{T} \rangle = 0$ has been imposed. Further for the N = Z even-even nuclei only T = 0 pairing solutions are discussed from physical grounds. The major results of the work are as follows: 1) Pairing favors axially symmetric solutions in Mg^{24} (prolate) and S^{32} (oblate). The inclusion of pairing correlations restore the energy gap for the axially symmetric solution which is essential for the stability of any single particle basis. Further the pairing energy along with the gain in the rotational energy due to the decrease of the moment of inertia make the ground state energies ($E_{J=0}$) of the axially symmetric state comparable to that of the axially asymmetric state even in the first order. In view of the somewhat smaller energy gap the axially symmetric solution may also be expected to gain more second order potential energy. 2) With the inclusion of pairing for Mg^{24} and S^{32} the overall picture for the cranking moment of inertia seems to be in a better agreement with experiment. The overestimate of the moment of inertia parameter ($A = \hbar^2/2\Im$) found in all the cases is encouraging in view of Peierls' correction to cranking. 3) For Ar^{36} we have shown that the pairing correlation favors the prolate state. Moreover, deformation of the prolate state is decreased considerably by the pairing correlations. Thus the moment of inertia decreases to the extent that the energy of the 2+ rotational state becomes higher than the expected energy of the 2+ vibrational state. Ar^{36} therefore seems to belong to the group of transitional nuclei. Experimentally Ar^{36} shows a vibrational spectrum with large anharmonicity characteristic of a transitional nucleus. The oblate state which corresponds to a $\Delta = 0$ solution of the HFB equation does not agree with experimental data as already point out.

Many questions, however, remain open. The role of the realistic forces and an extended basis has to be examined. In particular, it is well known that the tensor forces play an important role in determining the strength of the effective T = 0 central force which is important for the isospin pairing field. In this extended scheme one should calculate the binding energy to at least the second order for a choice between the various HFB solutions.

A detailed study of the one and two quasiparticle spectra including the rotation particle coupling will be important. Also it will be interesting to see how the T = 1 and higher T excited states are to be described, i.e., are they two or more quasiparticle states or does one have to generate them by constraining the isospin to take on prescribed values when solving the HFB equation. Some of these questions are expected to be answered in the near future.

ACKNOWLEDGMENTS

The authors wish to thank Professor Leonard Kisslinger for helpful discussions and Mrs. M. Ratner and Mr. P. S. Rajasekhar for valuable programming assistance. One of us (J.B.) wishes also to thank Prof. N. Glendenning and the Department of Nuclear Chemistry of Lawrence Radiation Laboratory for their kind hospitality at the LRL during summer 1968.

FOOTNOTES AND REFERENCES

*This work was performed under the auspices of the U. S. Atomic Energy Commission.

†Supported by NSF.

**Present address: University of Oregon, Eugene, Oregon.

1. S. G. Nilsson, Kgl. Danske Videnskab. Selskab. Mat. Fys. Medd. 29, No. 16 (1955).
2. M. G. Redlich, Phys. Rev. 110, 468 (1958).
3. F. Villars, Lectures in Proceedings of Enrico Fermi International School of Physics (Academic Press Inc., New York, 1963).
4. I. Kelson, Phys. Rev. 132, 3189 (1963).
5. I. Kelson and C. A. Levinson, Phys. Rev. 134, B269 (1964).
6. J. Bar-Touv and I. Kelson, Phys. Rev. 138, B1035 (1965).
7. M. K. Pal and A. P. Stamp, Phys. Rev. 158, 924 (1967).
8. W. H. Bassichis, A. K. Kerman, and J. P. Svenne, Phys. Rev. 160, 746 (1967).
9. J. Bar-Touv and C. A. Levinson, Phys. Rev. 153, 1099 (1967).
10. J. Parikh, Phys. Rev. Letters 26B, 607 (1968).
11. A. Goswami and L. S. Kisslinger, Phys. Rev. 140, B26 (1965).
12. H. T. Chen and A. Goswami, Phys. Letters 24, B257 (1967).
13. A. Goodman, G. Struble, and A. Goswami, Phys. Letters 26, B260 (1968).
14. K. Dietrich, H. J. Mang, and J. H. Pradal, Phys. Rev. 135, B22 (1964).
15. A. Bohr and B. R. Mottelson, in numerous communications.
16. M. Baranger and K. Kumar, Nucl. Phys. A92, 608 (1967).
17. J. Bar-Touv and I. Kelson, Phys. Rev. 142, 599 (1966).
18. A. P. Stamp, Nucl. Phys. A105, 627 (1967).
19. M. Vijcicic and Flowers, Nucl. Phys. 49,
20. J. Bar-Touv and A. Goswami (to be published).
21. G. Crawley and G. Garvey, Phys. Rev. 160, 981 (1967).

22. R. Peierls and J. Yoccoz, Proc. Phys. Soc, (London), A70, 381 (1957).

23. B. Cujec, Phys. Rev. 136, B1305 (1964).

24. G. J. McCallum and B. D. Sowerby, Phys. Letters 25B, 109 (1967).

25. M. K. Banergee, (private communication).

26. A. Faessler et al. (to be published).

TABLE CAPTIONS

Table I. HFB solution corresponding to the axially symmetric prolate shape of Mg^{24}, axially symmetric oblate shape of S^{32}, and the axially symmetric prolate shape of Ar^{36}. For each nucleus the italicized number at the top represents the HF single particle energy in the final state of the HFB convergence. This is followed by the component of the single particle wave functions in the jm representation (in the order: $d^{5/2}_{5/2}$, $d^{1/2}_{5/2}$, $d^{1/2}_{3/2}$ $s^{1/2}_{1/2}$, $d^{-3/2}_{5/2}$, $d^{-3/2}_{3/2}$). This is followed by the BCS amplitudes u_α and $\mathrm{Im}(v'_\alpha)$ corresponding to T = 0 pairing. The order parameter Δ_α is given next. The quasiparticle energy for the level α is shown last in the column also in italics. The expectation value of the Hamiltonian is shown split into two parts, E_{HF} and $E_{pairing}$. The chemical potential λ and the expectation values of the quadrupole Q_{20} and Q_{40} are also given (the Q_{20} and Q_{40} are given in arbitrary units). O^{17} single particle energies are used.

Table II. The spherical solution for Ne^{20} displaying combined T = 0 and T = 1 pairing. The axially asymmetric HF solution went to this solution when the pairing correlations were selfconsistently included. The single particle energies are those used in Ref. (6). Each column represents a jm state. The first number in each column is the HF energy by $v_p(\alpha)$, Re $v_{np}(\alpha)$, Im $v_{np}(\alpha)$, the total occupation $v^2(\alpha)$, $\Delta_p(\alpha)$, $\Delta^{T=1}_{np}(\alpha)$, $\Delta^{T=0}_{np}(\alpha)$, the gap parameter $\Delta(\alpha)$, and the quasiparticle energy E_α. All quantities have been defined in Sect. III.

Table III. Change of the HF wave function and energy due to the HFB correlations for the axially symmetric oblate state of S^{32} and prolate state of Ar^{36}. The first column gives the pure HF single particle basis. The second column gives the HF single particle basis in the final HFB solution.

i.e., with HFB occupation numbers. In each column the HF single particle energy is shown first in italics followed by the wave function in the representation of Table I. O^{17} single particle shell model energies are used.

Table IV. Variation of properties of the selfconsistent field with the single particle $\ell \cdot s$ force strength $\alpha_{\ell \cdot s}$ for Mg^{24}. The dispersion is defined as $\sum_{\substack{\alpha \\ \varepsilon_\alpha > \lambda}} v_\alpha^2$. ΔE_{HF} is the reduction of the HF energy due to the dispersion and A is the inertial parameter defined as $A = \hbar^2/2\Im$. The unit of energy is the MeV.

Table V. Cranking moment of inertia parameters ($A_i = 1/2\ \Im_i$ in MeV) of the axially asymmetric HF solutions and the HFB axially symmetric solutions for Mg^{24} and S^{32}. In each case the first values presented correspond to O^{17} single particle energies and the second to the single particle energies of Ref. (6).

Table I.

Mg^{24}	S^{32}	Ar^{36}
-17.882	-20.281	-23.012
0	0	0
.678	.119	- .616
- .289	.001	.080
- .676	.993	.783
0	0	0
0	0	0
.111	.128	.001
- .994	.992	.999
1.473	1.512	.008
6.659	5.950	6.979
-12.242	-19.840	-21.659
0	0	0
0	0	0
0	0	0
0	0	0
.965	.982	.989
.262	.191	.150
.581	.142	.001
.814	-.990	.999
2.494	1.554	.235
2.636	5.536	5.449

(continued)

Table I. Continued.

Mg^{24}	S^{32}	Ar^{36}
-10.369	-18.025	-21.445
0	0	0
.659	.810	.787
.646	.578	.091
.385	- .098	.610
0	0	0
0	0	0
.819	.182	.030
.573	- .983	.999
2.793	1.343	.314
2.973	3.747	5.239
- 7.000	-16.790	-19.451
1	1	1
0	0	0
0	0	0
0	0	0
0	0	0
0	0	0
.994	.393	.280
- .110	- .919	.960
.987	2.371	2.065
4.499	3.278	3.838

(continued)

Table I. Continued.

	Mg^{24}	S^{32}	Ar^{36}
	- 5.419	-12.872	-17.159
	0	0	0
	- .326	0	- .022
	.707	0	.993
	- .628	0	- .119
	0	- .191	0
	0	.982	0
	.998	.891	.456
	- .056	.453	.890
	.673	2.272	1.311
	6.007	2.810	1.616
	- 2.599	- 9.565	-15.424
	0	0	0
	0	- .574	0
	0	.816	0
	0	.068	0
	- .262	0	- .150
	.965	0	.989
	.997	.991	.844
	- .081	.137	.536
	1.440	1.398	1.685
	8.907	5.154	1.861
$\langle H \rangle_{HF}$	-71.508	-173.600	-232.929
$\langle H \rangle_{Pair}$	- 5.832	- 5.231	- 3.729
$\langle H \rangle$	-77.340	-178.831	-236.658
λ	-11.389	-14.526	-16.215
$\langle Q_{20} \rangle$	15.311	-19.533	4.046
$\langle Q_{40} \rangle$	- 5.377	-39.001	- 3.432

Table II.

$d_{5/2}^{-3/2}$	$d_{5/2}^{1/2}$	$d_{5/2}^{5/2}$	$s_{1/2}^{1/2}$	$d_{3/2}^{1/2}$	$d_{3/2}^{-3/2}$
-10.654	-10.584	-10.519	- 6.235	- 4.065	- 3.916
.373	.272	.196	.058	.069	.057
.373	.272	.196	.058	.069	.057
.142	.417	.528	.000	.005	.018
.300	.321	.355	.007	.010	.007
.783	.723	.693	.570	.995	.827
.783	.723	.693	.570	.995	.827
.302	1.128	1.891	.000	.073	.266
1.148	1.523	2.130	.806	1.409	1.199
1.255	1.628	2.224	4.991	7.234	7.343

$\langle H \rangle_{HF} = -34.618$ $E_{Pair} = -5.119$ $E_{total} = -39.737$

$\lambda = -11.160$

Table III.

S^{32}		Ar^{36}	
HF	HF (with HFB occupation)	HF	HF (with HFB occupation)
- 20.416	- 20.280	- 23.677	- 23.012
0	0	0	0
.071	.118	.739	.616
.002	.000	- .103	- .080
.997	.993	- .666	- .783
0	0	0	
0	0	0	
- 20.001	- 19.791	- 22.060	- 21.659
0	0	0	0
0	0	0	0
0	0	0	0
0	0	0	0
.978	.981	.980	.989
.209	.193	.198	.150
- 18.269	- 17.991	- 21.575	- 21.445
0	0	0	0
.805	.809	.673	.787
.591	.581	.150	.091
- .058	- .096	.724	.610
0	0	0	0
0	0	0	0

(continued)

Table III. Continued.

S^{32}		Ar^{36}	
HF	HF (with HFB occupation)	HF	HF (with HFB occupation)
- 16.257	- 16.738	- 18.414	- 19.451
1.	1.	1.	1.
0	0	0	0
0	0	0	0
0	0	0	0
0	0	0	0
0	0	0	0
- 12.848	- 12.866	- 17.528	- 17.159
0	0	0	
0	0	- .026	- .022
0	0	.983	.993
0	0	- .180	- .119
- .209	- .193	0	0
.978	.981	0	0
- 9.416	- 9.533	- 14.897	- 15.425
0	0	0	0
- .589	- .577	0	0
.807	.814	0	0
.040	.068	0	0
0	0	- .198	- .150
0	0	.980	.989
$\langle H \rangle_{HF}$ = -177.293	-172.926	-235.966	-232.933

Table IV.

$\alpha_{\ell \cdot s}$	HF gap	Dispersion	Quasiparticle gap	ΔE_{HF}	E_{Pair}	A_{HF}	A_{HFB}
-1.2	0.550	0.408	6.144	2.957	-7.426	0.098	0.318
-1.6	1.111	0.367	5.988	3.317	-6.812	0.111	0.305
-2.0	1.712	0.321	5.801	3.472	-6.031	0.123	0.286
-2.4	2.360	0.268	5.595	3.415	-5.108	0.134	0.265
-2.8	3.065	0.208	5.378	3.066	-4.007	0.146	0.242

Table V.

	Mg^{24}				S^{32}			
	Nonax.		Ax		Nonax.		Ax	
A_x	.338	.236	.281	.242	.387	.211	.223	.259
A_y	.182	.208	.281	.242	.509	.249	.223	.259
A_z	.389	.541	∞	∞	.471	.405	∞	∞

FIGURE CAPTIONS

Fig. 1. Occupation of the four-fold degenerate single-particle states of Mg^{24} for the HF, HFB (BCS) solutions and for the projected eigen-state of the total number operator.

Fig. 2. Moment of inertia parameter $\hbar^2/2\Im$ as function of the mass parameter for present HFB calculations. For comparison the HF results of Ref. (6) including the corresponding axially symmetric solutions of Mg^{24} and S^{32} and the average experimental values are shown.

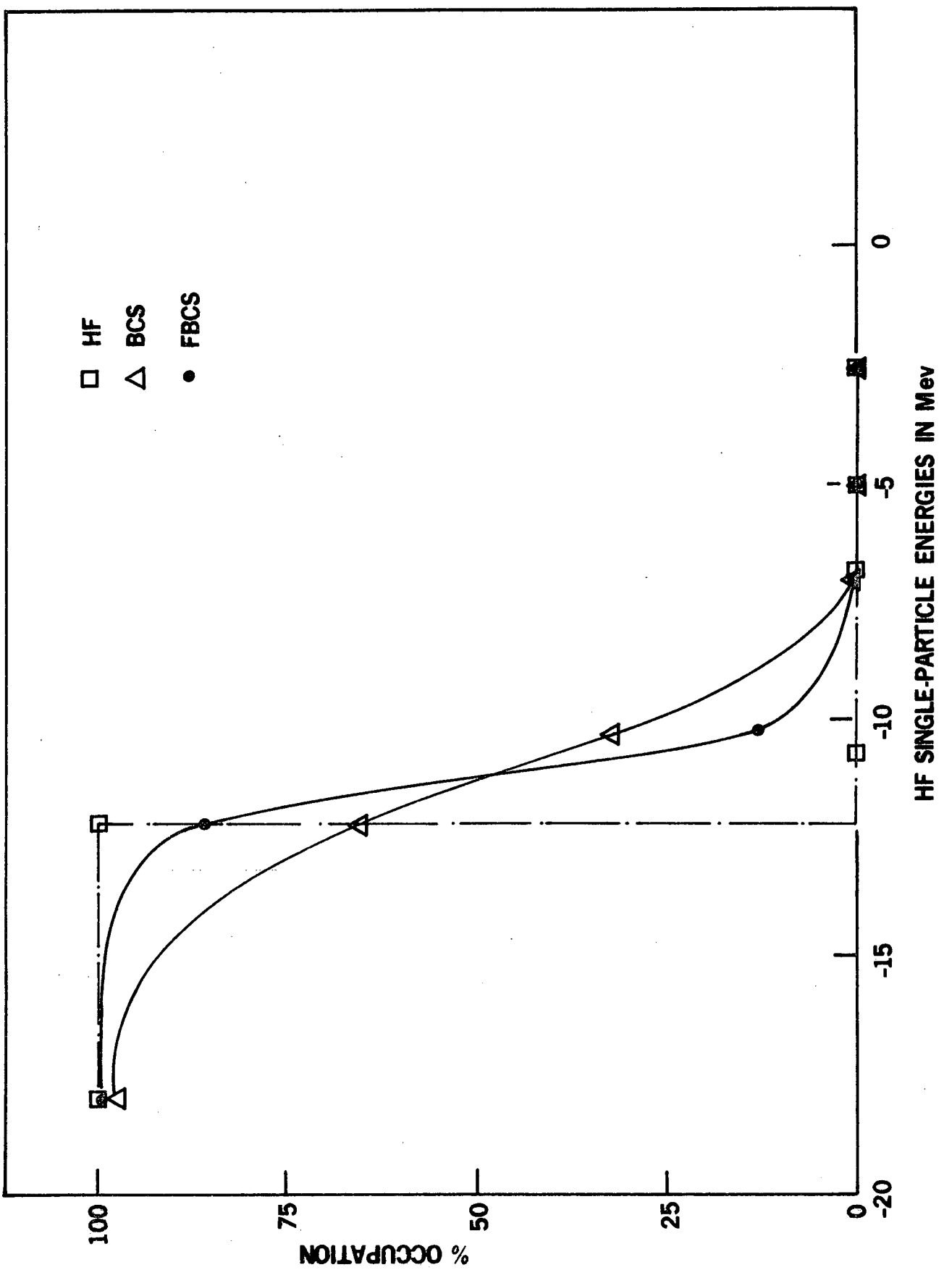
HF
BCS
FBCS
100
75
50
25
0
% OCCUPATION
0
-5
-10
-15
-20
HF SINGLE-PARTICLE ENERGIES IN Mev

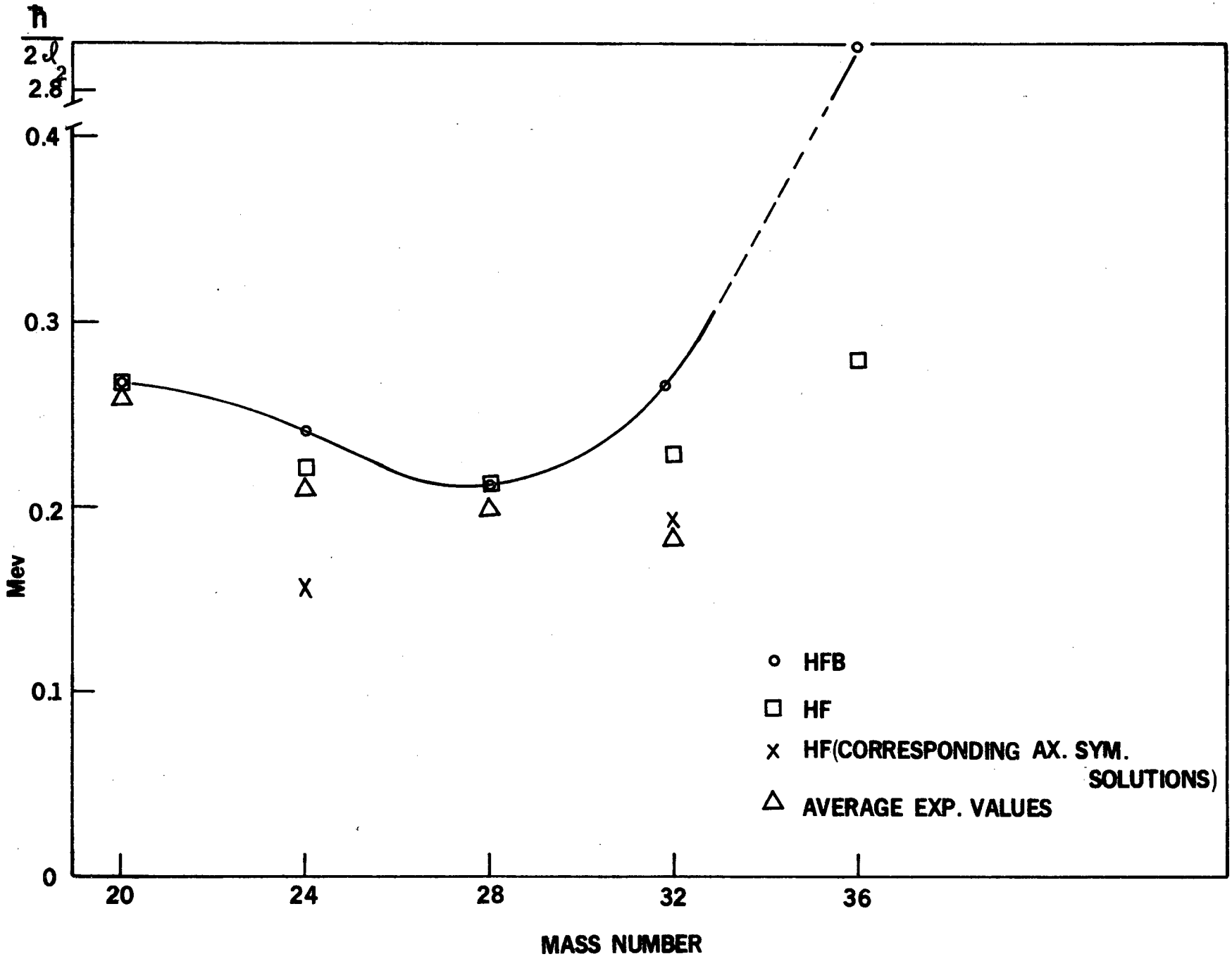
$\frac{\hbar}{2\mathcal{I}}$
2.8
0.4
0.3
0.2
0.1
0
Mev
20
24
28
32
36
MASS NUMBER
HFB
HF
HF(CORRESPONDING AX. SYM. SOLUTIONS)
AVERAGE EXP. VALUES